A Performance Analysis of a Tightly Coupled GPS/Inertial System for Two Integrity Monitoring Methods

Dr. Young C. Lee
Daniel G. O'Laughlin

The MITRE Corporation, Center for Advanced Aviation System Development (CAASD)
McLean, VA 22102

ABSTRACT

Use of an integrated GPS/inertial system can be effective in mitigating the effects of GPS signal interference such as intentional jamming. Currently the GPS/Inertial Working Group of RTCA SC-159 is developing requirements and test procedures for a tightly coupled GPS/inertial system. To support this Working Group, this paper investigates two of the key issues being addressed by the Working Group. The first issue is how well a tightly coupled GPS/inertial system can detect slowly growing errors. This paper investigates this issue for two integrity monitoring methods. The other issue relates to how long the system can coast upon complete loss of GPS signals caused by interference. Using analytic formulas, this paper determines maximum coasting times possible under various scenarios.

BIOGRAPHIES

Dr. Young C. Lee is a Lead Engineer in the Center for Advanced Aviation System Development (CAASD) at The MITRE Corporation in McLean, Virginia. He has been working in the area of GPS integrity since 1986, in support of the Federal Aviation Administration (FAA). Supporting the FAA's Satellite Operational Implementation Team (SOIT), he made major contributions towards the development of Technical Standards Order (TSO)-C129 and subsequent use of the GPS for aviation navigation. Over these years, he presented many papers at the Institute of Navigation (ION) conferences, some of which were published in *NAVIGATION, Journal of the ION*. He has also been actively participating in RTCA SC-159, currently serving as the secretary of the committee and as the chairperson of its Continuity Requirements Working Group. He received his B.S. from Seoul National University and Ph.D. from the University of Virginia, both in electrical engineering.

Daniel G. O'Laughlin is a member of the technical staff at MITRE/CAASD in McLean, Virginia. He has been performing GPS/WAAS system safety studies and GPS/Inertial modeling. He received his B.S. in Electrical Engineering from Worcester Polytechnic Institute and MSEE from Northeastern University.

INTRODUCTION

Since the early 1990s, the FAA has been applying a great deal of funding and effort to transition from the current ground-based navigation and landing system to satellite-based navigation using the Global Positioning System (GPS) and its augmentations in the National Airspace System (NAS). Recently, however, there are growing concerns regarding the robustness of the satellite-based navigation system. Of particular concern is that GPS and its augmentation (e.g., Wide Area Augmentation System (WAAS) and Local Area Augmentation System (LAAS)) signals are vulnerable to intentional and unintentional interference such that safety may be compromised. Augmenting GPS with an inertial system can be a very effective risk mitigation method.

Inertial systems have been used for decades by commercial airliners. In particular, they have been used as a sole means of navigation in transoceanic flights. An inertial system has almost no high frequency noise, but it can have large low frequency errors (bias errors) that grow with time. GPS, on the other hand, has high frequency noise but good long-term accuracy (i.e., small bias errors). Exploitation of such complementary characteristics is possible in the *tightly coupled* architecture where the GPS and inertial measurements are

integrated in the pseudorange domain in a full Kalman filter.

In spite of significant advantages of a tightly coupled GPS/inertial system, there has not been industry-wide standards for the avionics requirements and for the test procedures for certification of such a system. A tightly coupled GPS/inertial system called Autonomous Integrity Monitored Extrapolation (AIME) developed by Litton was certified as a primary means of navigation for up to the nonprecision approach (NPA) phase of flight on the Airbus 300 Series aircraft [1]. However, the system was certified on a special basis for a particular integrity monitoring method used by Litton. In order to develop Minimum Operational Performance Standards (MOPS) for requirements and test procedures for a tightly integrated GPS/inertial system, RTCA SC-159 formed a GPS/inertial Working Group in December 1997. While a GPS/inertial system could be effective in all phases of flight including precision approaches, the Working Group decided to focus, at least initially, on applications for up to NPA applications. In order to support the Working Group activity, this paper investigates two of the key issues addressed by the Working Group, which are described below.

The first issue is how well an integrated GPS/inertial system can detect failures causing a slowly growing error. This issue is part of a bigger issue of how one should handle different types of failures in developing requirements for a GPS/inertial system. Because an inertial system has almost no high frequency noise, it can detect rather easily a sudden drift. On the other hand, the system cannot easily detect a fault that causes a slowly growing error. This is because a Kalman filter used in an inertial system tends to adapt to and incorporate any slowly varying drift as a natural dynamic state (position error state or velocity error state). For this reason, a slowly growing error, while dragging off the solution, could easily escape detection. It is consequently a great challenge to be able to detect such slowly growing errors with a high probability (i.e., 0.999). While there is a general consensus among members of the RTCA Working Group that ramps in the range of 0.1 to 2 m/s are the worst case, there is no clear consensus regarding the question of whether a slowly growing error smaller than 2 m/s but larger than, say, 0.2 m/s can be detected with a required detection probability of 0.999 in the absence of redundant GPS satellites. To address this issue, this paper has performed an analysis for two integrity monitoring methods. The first method is called Solution Separation Method proposed by Honeywell in 1995 [2]. The other method is called Extrapolation Method, which has been implemented in AIME [1].

The second issue is a continuity issue as compared with the issue above, which is directly related to an availability issue. It relates to how long a tightly coupled GPS/inertial system can coast upon loss of all GPS signals while still maintaining certain accuracy. This coasting capability is one of the major benefits of a GPS/inertial system because continuing navigation, while maintaining desired accuracy upon occurrence of an otherwise hazardous situation, greatly improves safety of flight. This issue needs to be approached with caution because the answer depends on a variety of factors. This paper estimates the amount of error growth from different error sources as a function of time, using analytic formulas. From these estimates, the maximum coasting times are obtained under various scenarios.

The next section provides background material for the analysis that follows. The subsequent section presents a performance analysis of the two integrity methods. This is followed by an analysis of maximum coasting times. The last section provides conclusions and a discussion of further work. To support the analysis of maximum coasting times, the appendix at the end contains the equations used to estimate the amount of accumulating errors during a coasting period.

BACKGROUND

Parameters of Interest in Integrity Monitoring

Detection performance involves three basic parameters: test statistic, decision threshold, and Horizontal Protection Level (HPL). These parameters are described below.

Test Statistic vs. Decision Threshold

For a decision of whether to raise a flag or not to declare presence of a failure requires two quantities: a test statistic that is an observed quantity and decision threshold to compare the test statistic against. The selection of the test statistic depends on the individual integrity monitoring methods. Typically the decision threshold is chosen on the basis of statistical characteristics of the test statistic so that a false integrity alert (alert that occurs in a fault-free condition) occurs no more than at some specified rate, which is typically 10^{-5}/hr.

Horizontal Protection Level (HPL)

The HPL is an upper bound that a horizontal position error shall not exceed without being detected. If it is exceeded, it shall be detected with a 0.999 probability. In other words, a given integrity method must guarantee that a user position error, which is not a directly observable quantity, will be within the bound unless an integrity alert is raised. HPL is an important parameter that determines the availability of integrity function. That is, if HPL is less than the Horizontal Alert Limit (HAL) for a given

phase of flight (e.g., 0.3 nmi for NPAes), integrity function is available, and vice versa.

As much as it is important for an integrity method to detect any position error exceeding HPL with at least 0.999 probability, it is also important that HPL be small so that high availability may be provided. In order for availability to improve beyond what Receiver Autonomous Integrity Monitoring (RAIM) alone (without inertial aiding) can provide, HPL needs to be smaller than HAL as much as possible during RAIM holes (i.e., period during which RAIM is not available). This should be remembered for the discussion of the two integrity methods later on.

System Architecture

The system architecture that was used as the basis of our simulation model for a tightly coupled GPS/integrated system was one described in detail in [3] and illustrated in Figure 1. As shown, the system consists of three units: a GPS receiver, an Inertial Reference System (IRS), and an integration processor (IP). The IRS generates inertial solutions in an *open loop* mode and passes the information to the IP.[1] The GPS receiver generates the pseudorange (PR) measurements and satellite positions and passes these measurements on to the IP. Using these inputs from the GPS receiver and the IRS, the IP generates the corrections to the IRS solutions using a set of Kalman filters.

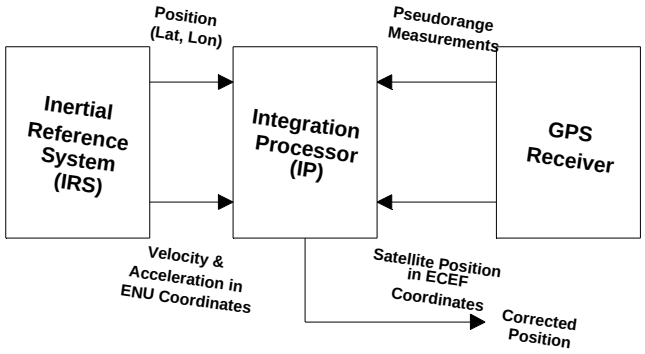

Figure 1. System Architecture for a Tightly Coupled GPS/Inertial System

In the Kalman filters of the IP, the measurement vector consists of the difference between two PRs to each satellite. One is the measured PR input from the GPS receiver. The other is the PR computed on the basis of the satellite positions obtained from the GPS receiver and the user location as calculated in the IRS. Using this measurement vector, the IP calculates the corrections to the inertial solutions and provides the integrity of the corrected solutions.

The IP first processes the measurement vector at a 1 Hz rate and pre-filters the data over every 2.5-min interval. With pre-filtering, most of the high frequency components in the measurements are removed. The remaining components of the measurements are modeled as satellite bias errors. The pre-filtered data is processed at the end of every 2.5-min interval by multiple Kalman filters running in parallel. One of these is a full-set filter, which processes data using a total of n GPS PR measurements. The others are subset filters, each of which processes data using a subset of (n-1) GPS PR measurements. These filters run in parallel so that when a full-set filter detects a failure, it can immediately identify the bad satellite by examining the test statistics in the subset filters and transitioning to the subset not containing the bad satellite.

The state vector consists of a total of 24 state variables: 12 inertial states, 2 clock states, 2 barometric states, and up to 8 states each of which represents GPS PR bias error. Process noise for the range bias error states is assumed to have zero mean and a standard deviation of 23 $m/\sqrt{hr}$ (bias component of Selective Availability (SA)). Measurement noise for the satellite range measurements is assumed to have zero mean and a standard deviation of 15 m (high frequency component of SA averaged over 2.5 min). The process for integrity monitoring performed in the IP is discussed next.

Two Integrity Methods

This subsection describes the two integrity methods. These methods assure the integrity of the corrected position solution by ensuring the GPS PR measurements are consistent and that their errors are within bounds.

Solution Separation Method

The Solution Separation Method is an extension of the RAIM concept applied to a GPS/inertial system. In this method, HPL is closely related to the decision threshold so that a probability of 0.999 may be guaranteed in detecting a position error exceeding the value of HPL regardless of the error growth rate. This method is briefly described below. A detailed description can be found in [2].

Test statistics. The test statistics of this method are the horizontal separations between the full-set and subset solutions.

[1] That is, there is no correction to the IRS solution fed back to the IRS, either from the Integration Processor or from the GPS receiver.

Decision threshold. First, the decision threshold (D_n) for the n^{th} test statistic (i.e., separation between the full-set solution and the n^{th} subset solution) is calculated from the Kalman filter covariance matrix P as follows:

- Calculate the matrix P for the solution separation between the full-set solution and the n^{th} subset solution.
- Calculate the standard deviation (σ) of the solution separation from the matrix P along the major axis of the horizontal separation distribution.
- $D_n = c \cdot (\sigma)$

  where c is a scalar that ensures that the false alert rate will not exceed a certain specified rate (10^{-5}/hr or equivalently, 0.333 x 10^{-6}/sample, assuming a correlation time constant of 2 min for the samples).

The above three steps are repeated for each n. If any of the test statistics exceeds the corresponding decision threshold, a flag is raised to declare the presence of a fault.

HPL. The HPL is based on two quantities: D_n and A_n. D_n is the decision threshold described above. A_n is an error bound that contains the n^{th} subset position error with a probability of 0.999 in a fault-free condition. A_n is calculated as follows:

- Calculate the covariance matrix P for the n^{th} subset.
- Calculate the standard deviation (σ) of the n^{th} subset position error along the major axis of the horizontal error distribution.
- Multiply σ by 3.09, a scalar corresponding to a missed detection probability of 0.001 in a normal distribution with a zero mean.

HPL is then obtained by

$$HPL = \max (D_n + A_n)$$

This HPL bounds the full-set solution error, guaranteeing a detection probability of 0.999.

In this method, the decision threshold and HPL formulas together guarantee, on an analytical basis, 0.999 detection probability for a given HPL regardless of the type of failure. For this reason, no extensive simulation is required to verify the detection performance. However, as will be seen later, HPL with this method tends to be relatively large so that a dramatic improvement in availability cannot be expected.

Extrapolation Method

This method was devised to detect slowly growing errors by observing the GPS measurements over a relatively long period (up to 30 min). Since this method is described in detail in [4], it is only briefly summarized below.

Test statistics. A standard equation for updating the state vector x in a Kalman filter is given by

$$x^{+}(k) = x^{-}(k) + K(k)\, r(k)$$

where

K(k): Kalman gain and

$r(k) = z(k) - H(k)x^{-}(k)$

r(k) is often called "innovation" and, as will be seen, it is very effective in detecting relatively fast growing errors. The Extrapolation Method uses three test statistics all based on innovations. The first one (s_1) is based on the innovation over the current cycle of 2.5 min duration and the other two, s_4 and s_{12} are obtained by averaging the innovations over 4 cycles (10 min) and 12 cycles (30 min), respectively.

It can be shown that all of the three statistics have a standard chi-square distribution with a degree of freedom equal to the number of satellites used [4]. Whether it is a central or non-central chi-square distribution depends on the absence or the presence of a range bias error.

Decision threshold. The decision threshold is derived from the Chi-square distribution and on the basis of the maximum allowable false alarm rate of 10^{-5}/hr or equivalently, 0.333 x 10^{-6}/sample in a fault-free condition.

HPL. In the Extrapolation Method, HPL is based on three quantities, HPL1, HPL2, and HPL3:

HPL1 = 5.33 $\cdot$ (σ value of position estimate uncertainty)

where the σ value is determined from the elements for the horizontal position error of the covariance matrix. This parameter relates to the rare normal performance with a 10^{-7} probability.

HPL2 is the maximum of the horizontal separation between the full-set and subset solutions. Note that HPL2 is the same quantity as that used for the test statistic in the Solution Separation Method. While HPL2 would remain small in a fault free condition, a large error caused by a failure would push up the value of HPL through HPL2. By increasing the HPL, this parameter reduces the possibility of an undetected position error exceeding the HPL.

HPL3 is derived in a manner similar to one for RAIM HPL calculation. First, ramp errors of unit size starting at the previous cycle are emulated on each satellite, one at a time, and their effect on the position error plus their effect on the test statistic are calculated. The maximum ratio of the position error and test statistic is then multiplied by a parameter called pbias to get HPL3. The parameter pbias

is the square root of the non-centrality parameter of the chi-square distribution that would make the missed detection probability of the assumed ramp error equal to 0.001 (See [5]). This parameter is an attempt to determine the effect of a ramp error on the position estimate.

HPL is then obtained by

HPL = root-sum-square (max (HPL1, HPL2), HPL3)

While each of the three parameters is an attempt to set the HPL large enough so that HPL can bound the position error with a 0.999 probability of detection, one can see that the HPL formula for the Extrapolation Method is still *ad hoc*. That is, one cannot show analytically whether the HPL formula indeed gives an upper bound such that a position error will not exceed it without being detected with a 0.999 probability. Therefore, the integrity performance of this method must be verified by means of very extensive simulation runs. This is a major drawback of the Extrapolation Method.

PERFORMANCE OF A TIGHTLY-COUPLED GPS/ INERTIAL SYSTEM IN THE PRESENCE OF A SLOWLY INCREASING ERROR

This section presents the analysis of the performance of the Solution Separation and Extrapolation Methods in detecting a failure causing a slowly increasing ramp error.

Scenarios for the Simulation

Simulations were run under the following test scenarios:

- GPS constellation
  - Optimized 24-Satellite Vehicle (SV) constellation as defined in Appendix B of the RTCA/DO-229 MOPS [6], with all SVs operating except during the period of RAIM holes, which were created by purposely removing 2 or 3 SVs
- Flight time prior to a RAIM hole
  - One hour (This was to attain a steady state with the GPS/Inertial system before an adverse event occurs)
- RAIM holes
  - Different RAIM holes were created that would last approximately one hour
- Ramp error start time
  - Variable:
    - Before RAIM hole starts
    - At the time the RAIM hole starts
    - After RAIM hole starts
- Ramp error size (m/s)
  - 0.1, 0.2, 0.5, 1.0, 2.0
- Turning maneuver during RAIM holes
  - Straight and level flight
  - 90-degree (deg) turn followed by a straight and level flight

Although numerous simulation runs were made, results are shown for only a representative set of these in Figures 2 through 8. In all cases the aircraft flew a straight and level flight path originating near Los Angeles (34N,118W) at a heading of 45 deg and a speed of 500 knots. For all figures in this section, results are plotted for the noise-free case. The noise-free case was used so that the performance of the Kalman filter affected by only the ramp error could be analyzed without the effect of random measurement noise.

Innovation

The innovation is shown in Figure 2 as a function of time for different ramp error rates with a RAIM hole induced by turning off SVs 19 and 22. Strictly speaking, the innovation r(k) is a vector. What is plotted in the figure is the most relevant element of r(k), i.e., the element

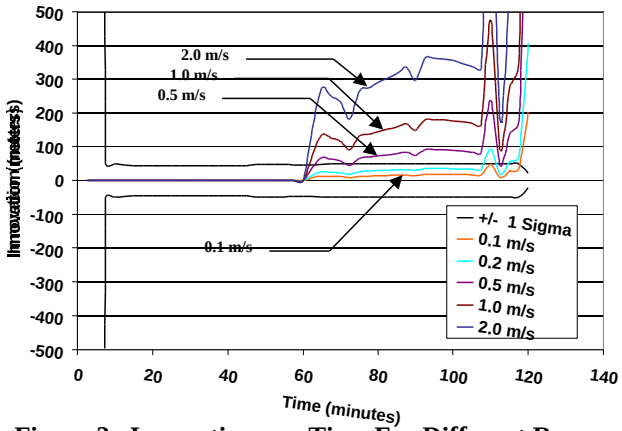

Figure 2. Innovations vs. Time For Different Ramp Error Rates

corresponding to that satellite causing an integrity failure. It is shown that in case of a relatively large ramp error size (e.g., 2 m/s), the innovation increases significantly beyond its 1-σ value so that presence of a failure becomes visible. On the other hand, in case of a slower ramp (e.g., 0.2 m/s or smaller), the innovation does not become much larger than a 1-σ or 2-σ value, thus making the failure not visible. In short, the innovation is effective in detecting relatively fast growing errors (e.g., ≥ 2 m/s) but is not as effective with slowly growing errors.

Plot for HPL Against Actual Position Error and Test Statistic Against the Decision Threshold

Figures 3a through 5b show HPL against actual position error and test statistic against the decision threshold for

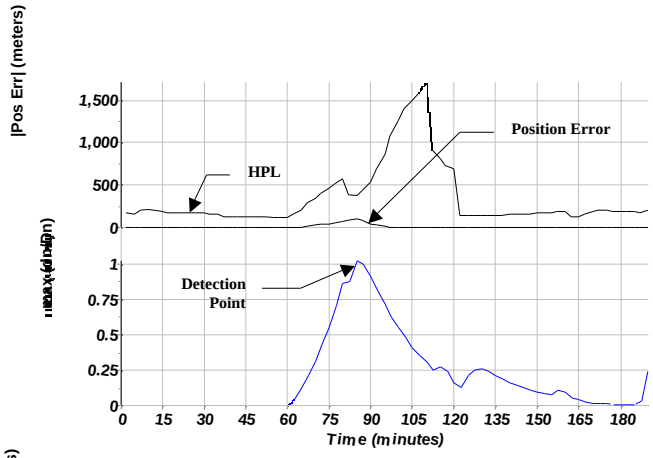

(a) Solution Separation Method

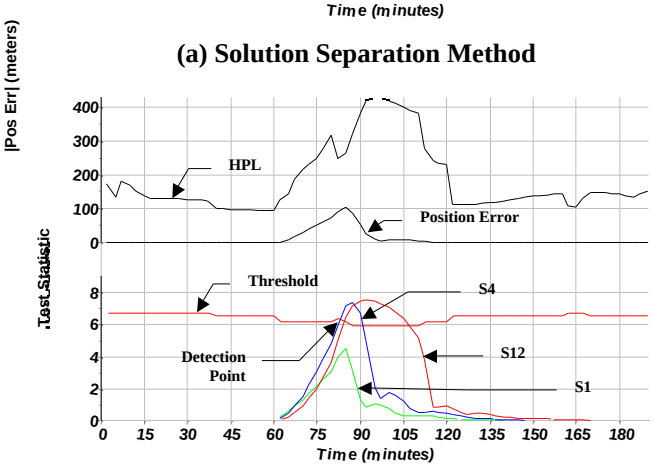

(b) Extrapolation Method

Figure 3. Position Error vs. HPL and Test Statistic vs. Threshold (0.1 m/s Ramp Error)

ramp errors growing at different rates of 0.1, 0.5, and 2.0 m/s for the two integrity methods. When a satellite is determined to be faulty, it is excluded from further use. In all cases we examined, shown and not shown in this paper, the bad satellite was always correctly identified to be excluded.

A RAIM hole was induced one hour into the flight by turning off SVs 19 and 22. At the same time, a PR ramp error was induced on SV 5. Typically, there were five satellites in view during the RAIM hole: four healthy satellites and the satellite with the ramp error. Not counting the satellite with the ramp error, there were five SVs in view between 60 minutes (min) and 82.5 min, six satellites at 85 min, five SVs again between 87.5 and 110 min, and six SVs between 110 min and 120 min. As soon as a failure is detected and the bad satellite excluded, one fewer satellite would be used. Note that all times reported in this section are with respect to the epoch time provided in Appendix B of the RTCA/DO-229 MOPS [6].

Figure 3 (a and b) is for a ramp error growing at a rate of 0.1 m/s. In this case, both methods detected the fault approximately 25 min after the ramp error began. The faulty satellite is identified and excluded. Therefore, from that point on until 110 min, there are only four SVs visible to the user. During this period, for the Solution Separation Method, shown in Figure 3a, the HPL grows to 1700 m. This is a result of degraded user-to-satellite geometry. Since the HAL for NPA is 0.3 nmi (555 m), NPA would not be available using this method for almost 45 min starting at about 80 min into the simulation run. For the Extrapolation Method, shown in Figure 3b, the test statistics averaged over a long time (e.g., the 10-min and the 30-min averages) exceed the decision threshold whereas the test statistic averaged over 2.5 min does not. The HPL eventually grows to exceed 400 m, significantly smaller than the maximum HPL for the Solution Separation Method. The growth in the HPL for the Extrapolation Method is due primarily to the component of HPL known as HPL2, which grows as the solution separation between the full-set and subset filters grow.

Figure 4 (a and b) is for a ramp error growing at a rate of 0.5 m/s. Both methods detected the fault approximately 10 min after the ramp error began. For the case of the Solution Separation Method, shown in Figure 4a, the HPL grows large with its maximum value exceeding 1800 m during the period when only four satellites are in view. For the Extrapolation Method, shown in Figure 4b, the HPL never exceeds 420 m, yet the position error never exceeded the HPL.

Figure 5 (a and b) shows the case with a ramp error growing at 2 m/s. Both methods are able to detect the fault within about 5 min after the ramp error begins. For the case of the Solution Separation Method, shown in Figures 4a, it is observed that the HPL again grows large with its maximum value exceeding 1800 m. For the Extrapolation Method, shown in Figure 5b, the HPL grows to exceed 900 m.

Analysis of Effect of Different Ramp Start Times on Performance

An analysis was also performed to determine the effect of different ramp start times in relation to the RAIM hole start time. For these cases, a worse RAIM hole than the cases described above was used. To generate the worse RAIM hole, three satellites were turned off (SVs 15, 19 and 22), thereby inducing a RAIM hole due to an insufficient number of satellites in view. In this case, there generally would be only three healthy satellites in view of the user during the RAIM hole, and one satellite (SV 5) with a ramp error.

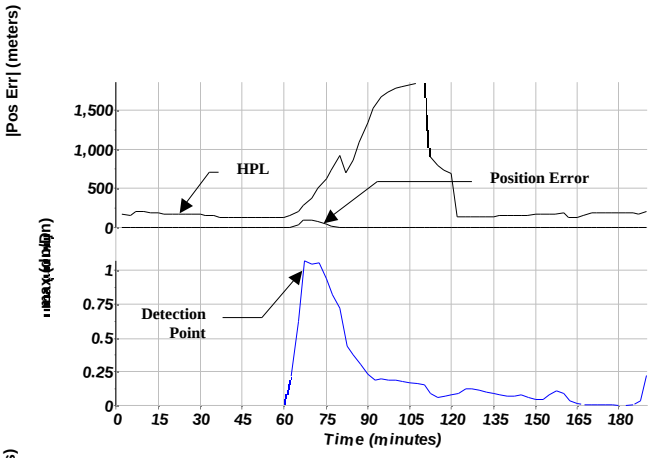

(a) Solution Separation Method

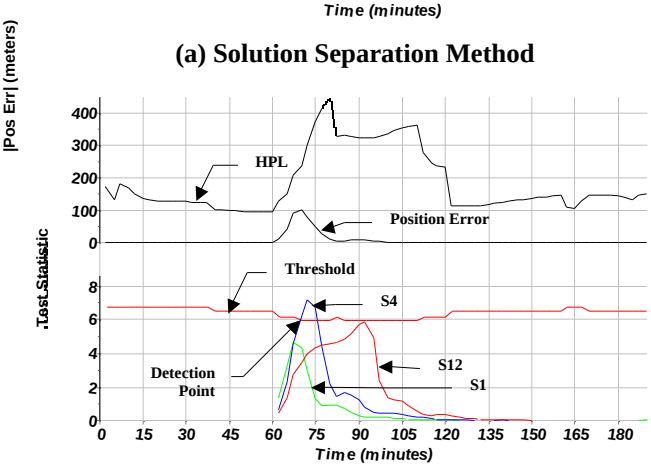

(b) Extrapolation Method

Figure 4. Position Error vs. HPL and Test Statistic vs. Threshold (0.5 m/s Ramp Error)

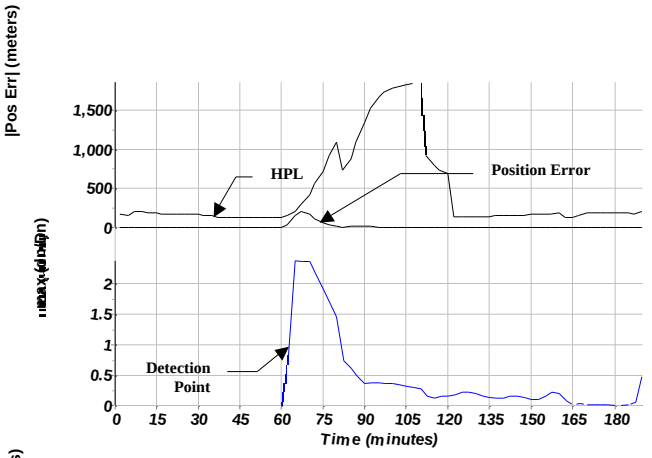

(a) Solution Separation Method

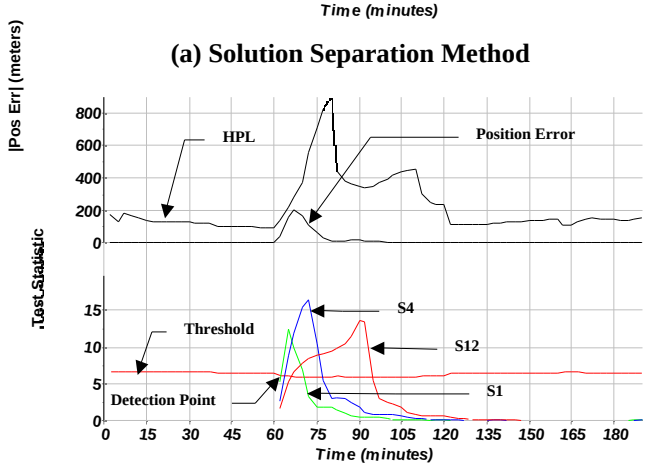

(b) Extrapolation Method

Figure 5. Position Error vs. HPL and Test Statistic vs. Threshold (2.0 m/s Ramp Error)

Figure 6 (a and b) shows the case where a ramp error starts 10 min before the RAIM hole begins. The size of the ramp error was set at 1.0 m/s. In this case, both methods were able to detect the satellite with the ramp error before the RAIM hole started. In the case of the Solution Separation Method, shown in Figure 6a, the satellite was excluded early but the HPL gets quite large, approaching 3800 m. The Extrapolation Method, shown in Figure 6b, was able to maintain an HPL of 1900 m. The reason the HPL grows to such a large number for both methods is because with only three healthy SVs in view, a GPS-only solution is not possible; therefore, position accuracy is determined primarily by the accuracy of the inertial system alone.

Figure 7 (a and b) shows the case where a ramp error starts 10 min after the RAIM hole. The size of the ramp error in this case was 0.5 m/s. The Solution Separation Method, shown in Figure 7a, was able to detect the failed satellite slightly earlier (32.5 min after the ramp error begins) than the Extrapolation Method did; nevertheless, the HPL has grown to 1800 m at the time of detection. For the Extrapolation Method, shown in Figure 7b, detection of the failed satellite occurs 40 min after the ramp error begins. Nevertheless, the position error is still bounded by the HPL, which at the time of detection has grown to 1600 m.

These results may indicate that both methods may suffer in their ability to detect failed satellites during periods of low (fewer than four) satellite visibility. This possibility requires further analysis.

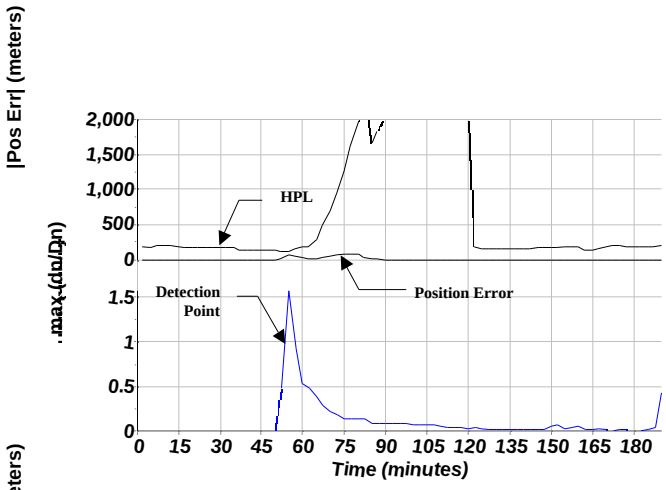

(a) Solution Separation Method

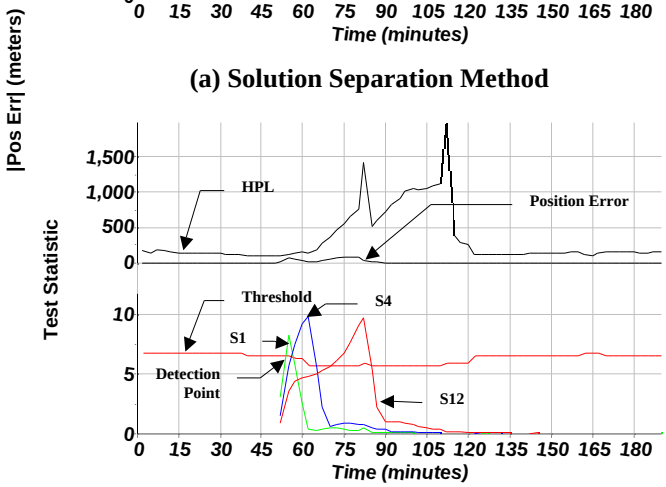

(b) Extrapolation Method

Figure 6. Position Error vs. HPL and Test Statistic vs. Threshold with 1.0 m/s Ramp Error Beginning at 50 Minutes (10 Minutes Before RAIM Hole)

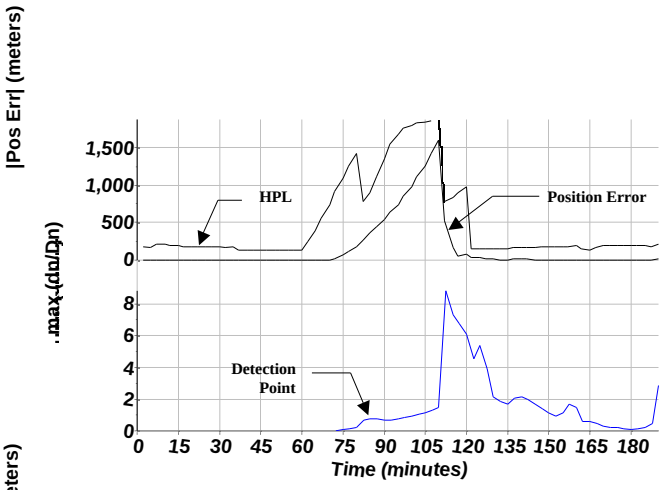

(a) Solution Separation Method

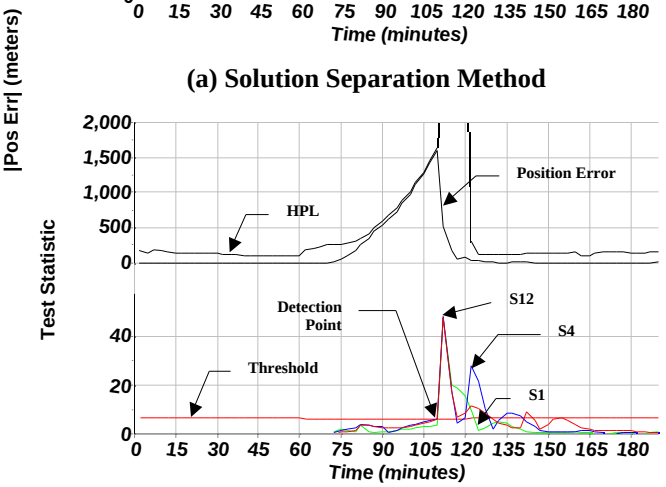

(b) Extrapolation Method

Figure 7. Position Error vs. HPL and Test Statistic vs. Threshold with 0.5 m/s Ramp Error Beginning at 70 Minutes (10 Minutes After RAIM Hole)

Comparison of HPLs for the Two Methods

As observed in the previous figures, the HPL for the Solution Separation Method becomes quite large. However, even in the fault-free case, the HPL for the Solution Separation Method is generally larger than the HPL for the Extrapolation Method. This is because the Solution Separation's HPL is greatly affected by the user-to-satellite geometry and the number of satellites in view. This is indicated in Figure 8, an example where there is no failed satellite but there is a RAIM hole between 60 min and 120 min. The Solution Separation Method's HPL exceeds 550 m during the RAIM hole, while the Extrapolation Method's HPL never exceeds 250 m. Thus, the Extrapolation implementation will generally have higher availability than the Solution Separation implementation.

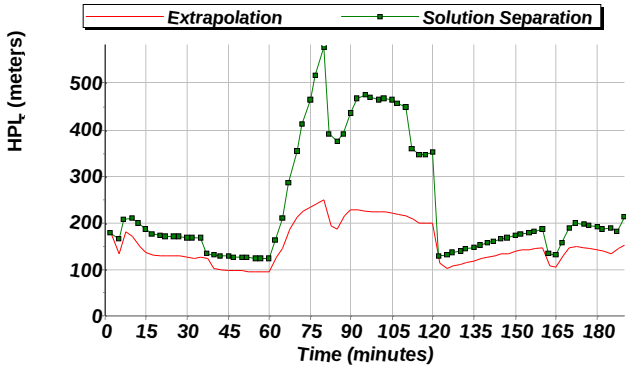

Figure 8. Comparison of HPLs for the Two Methods in the Fault Free Case

Summary of the Performance Analysis

The results of the performance analysis can be summarized as follows:

Innovation can be used to detect a failure causing a relatively fast growing error (e.g., 2 m/s). However, it cannot be effectively used to detect a failure causing slowly growing errors.

However, the test statistics for the Extrapolation Method, which averages the innovation vector elements over time, show it to be very effective. It is observed that the longer

it averages the innovations, the more effective it becomes in detecting a slower ramp. While the Solution Method guarantees satisfactory detection performance against HPL by theory, HPL tends to remain relatively large, thereby making it more difficult to obtain a high availability improvement.

Based on the observations discussed in this section, the two integrity methods are compared in Table 1. Advantages and disadvantages of each method are summarized along with their implications in real operations.

It was observed that the Extrapolation Method is very effective in detecting a failure, often raising a detection flag long before the position error exceeded the HPL. However, it remains a challenge to verify 0.999 detection probability. Litton reported that they had done a thorough simulation analysis to confirm satisfactory performance of the Extrapolation Method for certification of their AIME system. However, in spite of numerous simulation runs, it was not possible to confirm Litton's claim, which would have required a significantly larger number of runs.

Table 1. Comparison of Solution Separation Method and Extrapolation Method

	Solution Separation Method	Extrapolation Method
Advantages	Detection performance guaranteed on the basis of theory Performance does not depend on failure type	Can achieve sufficiently small HPL; thus dramatic improvement in availability is possible
Disadvantages	Cannot achieve sufficiently small HPL; thus dramatic improvement in availability is not possible	No good way to confirm detection performance based on theory; thus requires extensive simulation runs Performance depends on failure type
Under no failure condition	Relatively large HPL makes it more likely to generate "no integrity function available" during RAIM holes	Relatively small HPL makes it less likely to generate "no integrity function available"
Upon failure causing a relatively fast ramp error	Failure detected with a sufficiently high probability against HPL	Failure detected with a sufficiently high probability against HPL, which typically increases as the error increases
Upon failure causing a relatively slow ramp error	Failure detected with a sufficiently high probability against HPL	Failure detected with a sufficiently high probability except when a very slow undetected ramp (e.g., < 0.1 m/s?) lasts over a long RAIM hole (e.g., 1 hr)*

* In order for a failure to escape timely detection, the error must grow relatively slowly, and at the same time there are no redundant satellites (i.e., a RAIM hole). Since it will take a long time for such a slow error to grow to a sufficient magnitude, a missed detection occurs only when the failure lasts over a long RAIM hole. This may not be as much a problem as one might think. First, such a long RAIM hole is not likely with the current GPS constellation unless a significant number of satellites become inoperable. Second, the slower the ramp error, the more likely the GPS Control Segment will detect the failure before the magnitude becomes large enough to cause a problem.

ANALYSIS OF COASTING CAPABILITY

As was stated, one major potential benefit of an integrated GPS/inertial system is to be able to coast for some time after GPS signals are lost caused because of intentional and unintentional interference. This section analyzes how long a tightly integrated GPS/inertial system can coast upon a complete loss of GPS signals while maintaining navigation accuracy at a satisfactory level for a given phase of flight up to NPA. Several different factors that affect maximum coasting time are discussed below along with assumptions used in the analysis.

Factors Affecting Coasting Time and Underlying Assumptions

Several factors that affect coasting time are as follows**:**

- *Inertial sensor accuracy.* The quality of inertial sensors, especially the quality of the gyros, determines how well the inertial parameters calibrated by GPS measurements can be maintained during the coasting period. Our analysis has considered three different gyro qualities: 0.01, 0.1, and 1-deg/hr gyro bias error.
- *Gyro misalignment.* Gyro misalignment, that is, imperfect construction within an inertial measurement unit (IMU) assembly, allows both roll and pitch gyros to sense a fraction of the yaw rate, causing an attitude error about level axes. The attitude error, in turn, causes an acceleration error along the level axes. The gyro misalignment factor depends not on the quality of the gyro but on how well a factory calibration is performed with inertial sensors rigidly mounted together. As shown in Table 2, gyro misalignment of 10^{-5} radian was assumed for the navigation grade gyro and 10^{-4} radian for the others.
- *Accuracy of calibration of inertial parameters prior to loss of GPS signals.* The coasting time also depends on how well the gyro bias and the heading error are calibrated with GPS prior to loss of GPS signals. This calibration accuracy, in turn, depends on two factors:
  - Accuracy of GPS signal source for calibration of inertial parameters
    - GPS signals on a single frequency (L1) with SA on are assumed in our analysis.
  - Aircraft maneuver

Table 2. Gyro Sensor Accuracy and Gyro Misalignment

Quality of the Gyro	Gyro Noise (Angle Random Walk)	Gyro Bias Drift over One Hour (1)	Gyro Misalignment
Navigation Grade (0.01 deg/hr)	0.001 deg/√hr	0.005 deg/hr	10^{-5} rad
Mid-range (0.1 deg/hr)	0.01 deg/√hr	0.05 deg/hr	10^{-4} rad
Low-cost (1 deg/hr)	0.1 deg/√hr	0.5 deg/hr	10^{-4} rad

Note:
1. This is a typical gyro bias drift over an hour caused by temperature change.

  - An aircraft turning maneuver prior to loss of GPS signals allows more accurate calibration of gyro bias and heading error than without a maneuver. In our analysis, it is assumed that there was an aircraft maneuver within one hour prior to the loss of GPS signals.[2] The values in Table 2 above for the gyro bias drift are based on this assumption.

· *Aircraft maneuver during the coasting period.* An aircraft turn causes an additional position error increasing in time in the presence of heading error or gyro misalignment. Four different cases are analyzed:
  - A straight and level flight
  - A 90-deg turn followed by a straight and level flight
  - A 180-deg turn followed by a straight and level flight
  - A complete 360-deg turn followed by a straight and level flight

· *Aircraft speed.* The aircraft speed affects coasting time in two ways:
  - The gravity anomaly, which is the dominant source of acceleration noise, has a magnitude of ± 5 arc-s, or equivalently 25 μg (1-σ) and a typical correlation distance of 20 nmi. The correlation time for the gravity anomaly is obtained by dividing the correlation distance by the aircraft speed.
  - In the presence of a heading error, a change in the aircraft speed caused by a turn causes a cross track position error that grows at a rate proportional to the change of the aircraft speed.

[2] This assumption may not be valid for oceanic navigation or transcontinental en route navigation. However, in these cases, the navigation accuracy to maintain is much less stringent than the ones being considered in this analysis so that the assumption is no longer critical.

In our analysis, the following aircraft speeds are assumed.

Table 3. Aircraft Speed Assumed in Calculating Correlation Time of Gravity Anomaly Noise

Phase of Flight	Commercial Aircraft	GA Aircraft
NPA	180 knots	120 knots
Terminal	240 knots	150 knots
En Route	360 knots	150 knots

· *Accuracy to maintain during the coasting period.* For the accuracy to be maintained during the coasting period, three accuracy values are used: 0.3 nmi, 1 nmi, and 2 nmi (95 percent). These roughly correspond to the required navigation performance (RNP) values for the NPA, terminal, and en route phases of flight, respectively.

Position Error Growth from Different Error Sources During a Coasting Period

For the estimation of the maximum coasting time for a given scenario, we first estimate the position error that accumulates over a selected duration of coasting.

The Appendix shows, using an example, the steps to follow to derive position error growth from different error sources during a coasting period. One can repeat these steps for different durations of coasting time until the maximum coasting time is obtained that still satisfies the navigation accuracy requirement. In our analysis, a coasting time is considered to be acceptable only if the total 2-σ error at the end of the coasting is less than 90 percent of the 95-percent position accuracy to maintain (e.g., 0.27 nmi for 0.3 nmi, 95 percent accuracy to maintain). The other 10 percent (e.g., 0.03 nmi) is reserved to cover any other errors unaccounted for, such as the additional error that may be introduced when the last calibration with a GPS update occurs more than an hour prior to the loss of GPS signals.

Coasting Time Analysis Results

The results are summarized in Table 4. The following observations are made.

· With a navigation-grade (0.01 deg) gyro, one can coast for 20 to 30 min, depending on what types of turning maneuver the aircraft makes, while maintaining the accuracy of 0.3 nmi, 95 percent.

· With a 1-deg/hr gyro, one can coast only for several min while maintaining the accuracy of 0.3 nmi, 95 percent. This is not likely to be adequate to get out of the area affected by the interference.

Table 4. Maximum Coasting Times Upon Complete Loss of GPS Signals with a Tightly Coupled GPS/Inertial System

Gyro Accuracy Gyro bias Gyro Misalignment	Accuracy to Maintain (95 %)	Straight Level Coast without a Turn	90-deg Turn Followed by Straight & Level Coast	180-deg Turn Followed by Straight & Level Coast
bias = 1°/hr misalignment = 10^{-4} rad	0.3 nmi	4.5 min (4.5 min)	1.5 min (2.5 min)	< 1 min (1 min)
	1 nmi	8.5 min (8.5 min)	4 min (6 min)	2 min (3.5 min)
	2 nmi	11 min (11 min)	5.5 min (9.5 min)	3 min (6.5 min)
bias = 0.1°/hr misalignment = 10^{-4} rad	0.3 nmi	12 min (11.5 min)	7 min (8.5 min)	4 min (5.5 min)
	1 nmi	20 min (20 min)	16 min (17 min)	10 min (12 min)
	2 nmi	27 min (27 min)	22 min (25 min)	13 min (20 min)
bias = 0.01°/hr misalignment = 10^{-5} rad	0.3 nmi	30 min (28 min)	26 min (26 min)	20 min (22 min)
	1 nmi	1 hr 35 min (1 hr 34 min)	1 hr 3 min (1 hr 12 min)	50 min (1 hr 5 min)
	2 nmi	3 hr 10 min (3 hr 7 min)	2 hr 22 min (2 hr 55 min)	1 hr 55 min (2 hr 25 min)

Notes:

1. Coasting times underlined are for commercial aircraft speeds, while those in parentheses are for GA aircraft speeds shown in Table 3.
2. In case of one complete 360-deg turn, the maximum coasting times would be much like the case of no turning maneuver.

Ideally, results such as those in Table 4 would be compared with requirements for coasting time upon encountering intentional or unintentional interference. Unfortunately, however, there currently exist no such requirements. If an aircraft speed is 180 knots, one can coast about 60 to 90 nmi with a 0.01 deg/hr accuracy gyro while maintaining 0.3 nmi (95 percent) accuracy. This may well be satisfactory. On the other hand, with a 0.1 deg/hr accuracy gyro, the aircraft can coast approximately 30 nmi or less, which is not likely to be sufficient to allow a pilot to fly to an area unaffected by the interference signal (e.g., below the line of sight/radio horizon of ground interferers/jammers). Coasting time with a 1-deg/hr accuracy gyro is definitely not satisfactory.

CONCLUSIONS AND DISCUSSION OF FURTHER WORK

As we enter the era of satellite-based navigation using GPS and its augmentations, the user community is concerned about safety in the use of GPS or GPS/WAAS as the only means of navigation in the cockpit because of the vulnerability of GPS signals to interference, especially intentional jamming. Use of an integrated GPS/inertial system can be a very effective risk mitigation method. Currently, the GPS/inertial Working Group of RTCA Special Committee (SC)-159 is developing requirements and test procedures for a tightly coupled GPS/inertial system to be used for en route, terminal, and NPA phases of flight. In order to support this Working Group, this paper has investigated two of the key issues being addressed by the Working Group.

The first issue is how well a tightly coupled GPS/inertial system can detect a failure causing a slowly growing error. This paper has analyzed two integrity methods: the Extrapolation Method implemented by Litton, and the Solution Separation Method proposed by Honeywell. The paper examines how the respective methods behave in terms of detection performance and Horizontal Protection Level (HPL), a parameter that determines availability of the integrity function. The analysis reveals that both methods have advantages and disadvantages. While the Solution Separation Method guarantees satisfactory detection performance against HPL derived on the basis of theory, the HPL values tend to be relatively large so that it cannot achieve significant availability improvement beyond what can be attained with RAIM alone (i.e., without inertial aiding). On the other hand, while the Extrapolation Method can achieve significantly higher availability improvement, there is no good way to confirm the detection performance based on theory; therefore, very extensive simulation must be used instead. Litton reported that they had done a thorough simulation analysis using many simulation runs to confirm satisfactory performance of the Extrapolation Method for certification of their AIME system. It was not possible to confirm Litton's claim, which would have required a significantly larger number of runs. However, it might be possible to find a way to determine an upper bound for the missed detection probability for the Extrapolation Method with a covariance analysis rather than the brute-force Monte-Carlo simulation. This would allow significant reduction in the amount of simulation work required for this method. Along with this idea, an idea is being explored of possibly using the two methods together synergistically so that the shortfalls of both methods may be overcome.

The second issue that has been investigated in this paper relates to how long a tightly coupled GPS/inertial system can coast upon loss of GPS signals. For this issue, analytic formulas have been used to calculate the error growth from various error sources during the coasting period under various scenarios. The analysis reveals that depending on what kind of turning maneuver is made, an aircraft with a tightly coupled GPS/inertial system using a navigation-grade inertial unit can coast for 20 to 30 min (while maintaining the accuracy of 0.3 nmi, 95 percent). On the other hand, with a 1-deg/hr gyro, the user can coast less than 10 min even for accuracy of 1 nmi, 95 percent.

APPENDIX: DERIVATION OF POSITION ERRORS THAT ACCUMULATE FROM VARIOUS SOURCES DURING A COASTING PERIOD—EXAMPLE CASE

This appendix shows how to derive the position error that accumulates over the duration of a coasting period using the following example:

- Tightly coupled GPS/inertial system
- Navigation grade inertial sensors
- Coasting
  - 90-deg turn followed by a straight and level flight
  - at 180 knots
  - for 26 min
- SA is on

First, detailed steps of the derivation are shown and then the results of the calculations are summarized. It is noted that some of the formulas used here can be found in [7], [8], or [9].

Detailed Steps of the Derivation of Position Errors

1. Horizontal Measurement noise Power Spectral Density (PSD), R:
   Filtered high frequency selective availability:
   $\sigma_F = 50$ (ft)
   Selective availability correlation time:
   $T = 120$ (s)
   HDOP = 1.5
   $R = (HDOP \cdot \sigma_F)^2 \cdot T = 6.75\ E5\ (ft^2 \cdot s)$
2. Acceleration errors
   a. Gravity Anomaly noise PSD, Q_A
   (velocity random walk)
   (Accelerometer noise is neglected.)
   Standard deviation of the noise:
   $\sigma = 25\ \mu g = 8.05E\text{-}4\ (ft/s^2)$
   Correlation time: T = 400 (s)
   (assuming gravity anomaly correlation distance = 20 nmi and aircraft speed of 180 knots)
   $Q_A = \sigma^2 \cdot T = 2.592E\text{-}4\ (ft^2/s^3)$
   b. Steady-state Kalman filter time constant, τ [7]:
   $\tau = (R/Q_A)^{1/4} = 225.90$ s (< 4 min)
   c. Steady-state Kalman filter variances
   $P_{11} = \sigma_{1A}^2 = \sqrt{2} \cdot Q_A \cdot \tau^3$
   $= 4.226E+3\ (ft^2)$; $2\sigma_{1A} = 130.0$ (ft)
   $P_{22} = \sigma_{2A}^2 = \sqrt{2} \cdot Q_A \cdot \tau$
   $= 8.281E\text{-}2\ (ft^2/s^2)$;
   $2\sigma_{2A} = 5.755E\text{-}1$ (ft/s)
   d. Two sigma position errors due to calibration error after coasting t = 26 min (1560 s):
   Position error due to position calibration error:
   $2\sigma_{PPA} = 2\ \sigma_{1A} = 130.0$ (ft)
   Position error due to velocity calibration error:
   $2\sigma_{PVA} = 2\sigma_{2A}/\omega_S \cdot \sin(\omega_S \cdot t) = 433.8$ (ft)
   (ω_S = Schuler frequency = 1.24E-3 (rad/s)
   e. Position error because of velocity random walk induced by gravity anomaly while coasting for
   t = 26 min [8]:
   $\sigma^2_{Arw} = (Q_A \cdot/2\omega_S^2) \cdot \{t - 1/2\omega_S \cdot (\sin 2\omega_S t)\}$
   $= 1.54E+5\ (ft^2)$;
   $2\sigma_{Arw} = 785.1$ (ft)
3. Gyro errors
   a. Gyro noise PSD, Q_G:
   $Q_G = (0.001\ deg/\sqrt{hr})^2$
   $= 8.7644E\text{-}11\ (ft^2/s^5)$
   (converted μrad to μg's)
   b. Steady-state Kalman filter time constant, t:
   $\tau = (R/Q_G)^{1/6} = 4.444E+2$ s
   c. Steady-state Kalman filter variances:
   $P_{11} = \sigma_{1G}^2 = 2 \cdot Q_G \cdot \tau^5 = 3.038E+3\ (ft^2)$;
   $2\sigma_{1G} = 110.2$ (ft)
   $P_{22} = \sigma_{2G}^2 = 3 \cdot Q_G \cdot \tau^3 = 2.308E\text{-}2\ (ft^2/s^2)$;
   $2\sigma_{2G} = 0.304$ (ft/s)
   $P_{33} = \sigma_{3G}^2 = 2 \cdot Q_G \cdot \tau = 7.790E\text{-}8\ (ft^2/s^4)$;
   $2\sigma_{3G} = 5.582E\text{-}4\ (ft/s^2)$
   d. Two sigma position errors after coasting for t = 26 min due to calibration error:
   Position error due to position miscalibration:
   $2\sigma_{PPG} = 2\sigma_{1G} = 110.2$ (ft)
   Position error due to velocity miscalibration:
   $2\sigma_{PVG} = 2\sigma_{2G}/\omega_S \cdot \sin \omega_S t = 229.0$ (ft)
   Position error due to angle miscalibration:
   $2\sigma_{PAG} = 2\sigma_{3G}/\omega_S^2 \cdot (1 - \cos \omega_S t) = 492.1$ (ft)
   e. Position error due to angle random walk induced by gyro noise while coasting for t = 26 min:
   $\sigma^2_{Grw} = Q_G/2\omega_S^4 \cdot \{3t - 4/\omega_S \cdot \sin \omega_S t + 1/2\omega_S \cdot \sin 2\omega_S t\}$
   $= 2.59E+4\ (ft^2)$;
   Therefore,
   $2\sigma_{Grw} = 321.8$ (ft)
4. Gyro bias calibration error, dGB_C:
   Assume gyro bias calibration due to temperature change over 1 hour:
   $dGB_C = 0.005$ deg/hr
   Position error due to gyro bias calibration error of 0.005 deg/hr after coasting for t = 26 min:
   $\sigma_{dGB_c} = g \cdot dGBc/\omega_S^3 \cdot \{\omega_S t - \sin \omega_S t\} = 409.1$ (ft)
   $2\sigma_{dGB_c} = 818.2$ (ft)
5. Error caused by the heading error present before a turn (σ_h)

σ_h = c * (1-σ Heading Error) * (aircraft speed in knots) * (t/60)
where

c = 1 for 90-deg turn,
= 2 for 180-deg turn
= 0 for 360-deg turn

1-σ Heading Error = 0.0005 rad (for 0.01-deg/hr gyro)
= 0.005 rad (for 0.1-deg/hr gyro)
= 0.025 rad (for 1-deg/hr gyro)

t = coasting time (min)

With a 90-deg turn followed by a straight and level flight for 26 min at a speed of 180 knots,

σ_h = (0.0005 rad) * (180 knots) * (26/60)
= 236.9 (ft)

6. Error caused by a gyro misalignment with an aircraft turn (σ_m)

σ_m = c * f * Re {1-cos(Wt)} [9]

where

c = 1 for 90-deg turn
= 2 for 180-deg turn
= 0 for 360-deg turn

f: misalignment factor

Re (Radius of the Earth) = 20.926E6 (ft)

W = √g/Re = 1.24E-3 /s

t: Coasting time (s)

For a 90-deg turn with a misalignment factor of 10^{-5},

σ_m = 10^{-5} * Re {1-cos(Wt)}
= 283.8 (ft)

Summary of the Calculations

Table A-1 summarizes the calculations done above as an example and shows the two-sigma value of the total error accumulating during the coasting period.

Table A-1. Total Two-Sigma Error with a 90-deg Turn Followed by a Straight and Level Flight for 26 Minutes (With Navigation-Grade Inertial Sensors and SA On)

Error Source	Error Components	2 σ error (ft)
Uncalibrated DC (bias) component of SA before coasting:	23 m, (1 σ) HDOP = 1.5	226.4
Total accumulated errors during the coasting period due to the initial Kalman filter errors caused by gravity anomaly	$2\sigma_{PPA}$ $2\sigma_{PVA}$	130.0 433.8
Error due to velocity random walk induced by gravity anomaly during coasting	$2\sigma_{Arw}$	785.1
Total accumulated errors during the coasting period due to the initial Kalman filter errors caused by gyro noise:	$2\sigma_{PPG}$ $2\sigma_{PVG}$ $2\sigma_{PAG}$	110.2 229.0 492.0
Error due to gyro angle random walk noise during coasting:	$2\sigma_{Grw}$	321.8
Kalman filter gyro bias calibration error:	$2\sigma_{dGB_c}$	818.2
Error caused by the heading error present before a turn	$2\sigma_h$	473.8
Error caused by a gyro misalignment with an aircraft turn	$2\sigma_m$	567.6
Total (2σ): **Root-sum square of all errors:**		**1580.9 ft (0.26 nmi)**

ACKNOWLEDGMENTS

The authors would like to acknowledge the Navigation Architecture and System Engineering Office (ASD-140), the sponsor of this work. The authors are grateful to Dr. John Diesel of Litton and Mr. Mats Brenner of Honeywell for their many helpful suggestions on our simulation analysis of the two integrity monitoring methods analyzed in this paper. The authors would also like to thank Mr. Ron Braff of MITRE/CAASD for his review of the draft of this paper and for his insightful comments

.

REFERENCES

1. Diesel, J. W., and G. Dunn, 17–20 September 1996, "GPS/IRS AIME: Certification for Sole Means and Solution to RF Interference," *Proceedings of ION GPS-9*6, Kansas City, MO, Institute of Navigation, Alexandria, VA.
2. Brenner, M., 1995, "Integrated GPS/Inertial Fault Detection Availability," *Proceedings of ION GPS-95*, Palm Springs, CA, September, 1995, Institute of Navigation, Alexandria, VA.
3. Diesel, J. W., and J. King, January 1995, "Integration of Navigation Systems for Fault Detection, Exclusion, and Integrity Determination—Without WAAS," *Proceedings of ION National Technical Meeting*, Anaheim, CA, Institute of Navigation, Alexandria, VA.
4. Diesel, J. W., and S. Luu, September 1995, "GPS/IRS AIME: Calculation of Thresholds and Protection Radius Using Chi-Square Methods," *Proceedings of ION GPS-9*5, Palm Springs, CA, Institute of Navigation, Alexandria, VA.
5. Brown, R. G. and G. Chin, 1998, "GPS RAIM: Calculation of Threshold and Protection Radius Using Chi-Square Methods—A Geometric Approach," Institute of Navigation Special Monograph Series, Vol. V, Institute of Navigation, Alexandria, VA.
6. RTCA SC-159, 8 June 1998, *Minimum Operational Performance Standards for Global Positioning System/Wide Area Augmentation System Airborne Equipment*, RTCA/DO-229A, RTCA Inc.
7. Diesel, J. W., 1987, "Integration of GPS/INS for Maximum Velocity Accuracy," *NAVIGATION, Journal of The Institute of Navigation*, Vol. 34, No. 3, Fall 1987, Institute of Navigation, Alexandria, VA.
8. Diesel, J. W., 1988, "GPS.INS Integration by Functional Partitioning," *Proceedings of the Satellite Division's International Technical Meeting*, Colorado Springs, CO, September 1988, Institute of Navigation, Alexandria, VA.
9. Farrell, J., R. Anoll, and E. McConkey, "IMU Coast: Not a Silver Bullet," *Proceedings of the 55th Annual Meeting*, Cambridge, MA, 28–30 June 1999, Institute of Navigation, Alexandria, VA.